# Directly Detected Nuclear Magnetic Resonance of Optically Pumped GaAs Quantum Wells

S. E. Barrett, R. Tycko, L. N. Pfeiffer, and K. W. West
*AT&T Bell Laboratories, 600 Mountain Avenue, Murray Hill, New Jersey 07974*
(Received 19 November 1993)

Optical pumping strongly enhances nuclear spin polarizations in an *n*-doped GaAs/AlGaAs multiple quantum well, allowing NMR signals of the GaAs wells to be investigated by direct, radio-frequency detection in a 7.05 T field. The optically pumped NMR signals exhibit unanticipated dependences on the pumping wavelength, polarization, and power. The temperature dependence of the $^{71}$Ga NMR Knight shift is consistent with a $g^*$ value of $-0.49 \pm 0.02$ for electrons in the wells, with no exchange enhancement. We present evidence that the doped and photoexcited electrons do not reach a common spin temperature under optical pumping.

PACS numbers: 73.20.Dx, 76.60.−k, 78.66.Fd

Nuclear magnetic resonance (NMR) spectroscopy is a powerful local probe of the electronic and structural properties of bulk materials. Unfortunately, the low sensitivity of directly detected NMR has severely limited its application in studies of microscopic samples (e.g., thin films, quantum semiconductor structures, and nanocrystalline materials). The NMR signal amplitude is proportional to the product of the number of nuclear spins $N$ and their average polarization $P_n \equiv \langle I_z \rangle$. $P_n$ is usually very small (e.g., typical nuclear spin splittings are $\sim 5$ mK in a 10 T field, making $P_n \sim 10^{-4}$-$10^{-5}$ in equilibrium at 100 K) so that direct detection of NMR signals in solids usually requires $N \geq 10^{17}$-$10^{20}$. Clearly, much smaller samples ($N \sim 10^{12}$-$10^{15}$) could be studied if the nuclear spins were completely polarized ($P_n \sim 1$). In this Letter, we describe experiments in which nuclear spins in a GaAs/AlGaAs multiple quantum well (MQW) structure are strongly polarized by optical pumping of interband transitions with near-infrared laser light. Optical pumping generates electrons and holes with nonequilibrium spin polarizations which then polarize the nuclei through electron-nucleus hyperfine couplings, i.e., by dynamic nuclear polarization (DNP) [1-3]. This optical pumping process has been studied extensively in the context of *optically detected* NMR (ODNMR) in GaAs-based samples [3-10]. We show that optical pumping allows the *direct radio-frequency detection* of NMR signals from the quantum wells, report measurements of the dependence of the optically pumped NMR (OPNMR) signals on the laser power, wavelength, and polarization, and describe measurements of NMR frequency shifts and spin-lattice relaxation times ($T_1$) made possible by optical pumping.

The MQW sample contains forty 300 Å wide GaAs wells separated by 3600 Å $Al_{0.1}Ga_{0.9}As$ barriers, grown by molecular beam epitaxy on a semi-insulating GaAs(001) substrate. Si delta-doping spikes are located in the centers of the barriers, yielding a carrier density $n_s = 6.3 \times 10^{10}$ cm$^{-2}$ in each well at 3.8 K, with mobility $\mu = 1.44 \times 10^6$ cm$^2$/Vs. The substrate was removed by chemical etching, ensuring that light was absorbed only in the wells in our experiments. The resulting 17 $\mu$m thick film (surface area $\approx 0.20$ cm$^2$) was affixed to a sapphire block with vacuum grease and mounted on the cold finger of a modified Janis Supertran-B cryostat in the 7.05 T field of a Bruker MSL 300 NMR spectrometer. An rf coil for NMR excitation and detection was wound around the sample through grooves cut in the sapphire block. Optical excitation was provided by a cw Ti:sapphire laser pumped by an $Ar^+$ laser. After transmission through an optical fiber, the laser light passed through a shutter controlled by the NMR spectrometer, a linear polarizer, a zero-order $\lambda/4$ waveplate ($\lambda = 780$ nm) and the quartz window of the cryostat. The waveplate was adjusted to provide $\sigma^+$,$\sigma^-$, or linearly polarized light at the sample, with $>95\%$ polarization in the 735-850 nm range. The magnetic field, the light beam, and the growth axis of the sample were all parallel. The laser spot size was $\sim 0.33$ cm$^2$ at the sample. Polarization-sensitive photoluminescence (PL) and photoluminescence excitation (PLE) spectra were obtained by collecting luminescence within 5° of the incident light and passing it through a $\lambda/4$ waveplate ($\lambda = 830$ nm), a linear polarizer, a Spex 0.22 m single monochrometer (1.2 nm resolution), and an amplified photodiode. The PL spectrum of the GaAs wells in the 7.05 T field shows a single peak at 817 nm, 4.3 nm wide (FWHM). The polarization of the luminescence at 817 nm, defined as the quantity $(I^+ - I^-)/(I^+ + I^-)$, is $-2.6\%$ for $\sigma^+$ and $-5.2\%$ for $\sigma^-$ excitation at 806 nm, 600 mW/cm$^2$, and 5.7 K.

All OPNMR measurements described below were carried out with the timing sequence SAT-$\tau_L$-$\tau_D$-DET, where SAT represents a train of twenty $\pi/2$ pulses separated by 1 ms that saturates (destroys) any polarization of the nuclear isotope of interest, $\tau_L$ is a period during which the light shutter is open, $\tau_D$ is a period during which the shutter is closed, and DET represents the detection of NMR free induction decay (FID) signals following a single $\pi/2$ pulse. If $\tau_D = 0$, OPNMR signals are detected with the shutter open; otherwise, signals are detected with the shutter closed.

Figure 1 shows $^{71}$Ga ($S=3/2$, rf carrier frequency of 91.566 MHz) NMR spectra of the MQW, obtained at 5.1 K. Figure 1(a) is an OPNMR spectrum obtained in 8 shots with $\sigma^+$ light ($\lambda=815$ nm, 120 mW/cm$^2$), with $\tau_L=30$ s and $\tau_D=1$ s. The signals arise primarily from the GaAs wells (see below). In addition to the intense central line at 231 ppm, weaker and broader "satellite" lines from the $m=\pm 1/2 \rightarrow m=\pm 3/2$ transitions of nuclei with quadrupole splittings of 15 kHz are visible. We infer from Fig. 1(a) that the signal-to-noise ratio per 300 Å well ($5.3\times10^{15}$ $^{71}$Ga nuclei) is $\sim$0.6 in a single shot. Figure 1(b) was obtained with $\tau_L=0$ and $\tau_D=31$ s (i.e., without optical pumping). There is no detectable signal because of the small, nearly equilibrium nuclear polarization of the wells and the very long $T_1$ in the barriers (see below). Figure 1(c) was obtained with $\tau_L=0$ and $\tau_D=5400$ s. In this case, since $\tau_D$ exceeds the barrier $T_1$ ($\sim$2500 s), all $^{71}$Ga nuclei in the sample ($N=2.7\times10^{18}$) make their thermal-equilibrium contributions ($P_n=0.0011$) to the spectrum. Comparison of the signal amplitudes in Figs. 1(a) and 1(c) indicates that the spin polarization of the nuclei in the wells is roughly $-0.033$ in Fig. 1(a), with the negative sign due to the inverted (emissive) nature of the OPNMR signal. We observe $^{69}$Ga and $^{75}$As OPNMR signals of comparable intensity under the conditions of Fig. 1(a).

The origin of the satellite lines visible in Fig. 1(a) is not fully understood. $^{69}$Ga OPNMR spectra of the GaAs wells show larger satellite splittings, scaling with the nuclear quadrupole moment. This confirms that the satellite lines are indeed due to quadrupole couplings and are not experimental artifacts. Our estimates of the electric field gradients due to strains produced in the GaAs wells by the slight lattice mismatch with the $Al_{0.1}Ga_{0.9}As$ barriers (using a point charge model) and of the field gradients due to the internal electric field produced by the modulation doping show these to be too small to produce the observed splittings. Nevertheless, the hypothesis that these satellites originate from a lowering of the cubic symmetry and a concomitant modification of the electronic structure near the well/barrier interface explains their weak intensity in Fig. 1(a) and their absence in Fig. 1(c).

Figure 2 shows the dependence of the OPNMR signal amplitude on the laser wavelength (OPNMR excitation spectrum) along with the PLE spectrum for both $\sigma^+$ [Fig. 2(a)] and $\sigma^-$ [Fig. 2(b)] excitation. The confinement of the electronic wave function inside the wells breaks the continuum of electron and hole states into subbands, and then the continuum of states along the well is further broken up into Landau levels by the applied field [11]. This structure in the density of states is reflected in absorption and PLE spectra, and we expect it to show up in OPNMR excitation spectra as well, since optical absorption is a prerequisite for optical pumping. Although there is some correlation between the PLE and OPNMR results near the band gap, the discrepancies become worse as the laser energy is increased, presumably be-

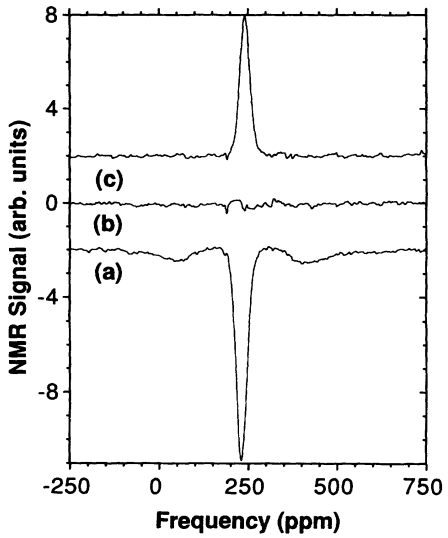


FIG. 1. $^{71}$Ga NMR spectra of the GaAs/AlGaAs multiple quantum well at 5.1 K. (a) 30 s of optical pumping after destruction of nuclear spin polarization ($\tau_L=30$ s, $\tau_D=1$ s). Signals are primarily from nuclei in the GaAs wells. (b) 31 s delay after destruction of spin polarization, no optical pumping ($\tau_L=0$, $\tau_D=31$ s). (c) 5400 s delay after destruction of spin polarization, no optical pumping ($\tau_L=0$, $\tau_D=5400$ s). Signals are primarily from nuclei in the AlGaAs barriers. All spectra have the same vertical scale but are offset for clarity. Frequencies are relative to a $1M$ $Ga(NO_3)_{3(aq)}$ reference signal.

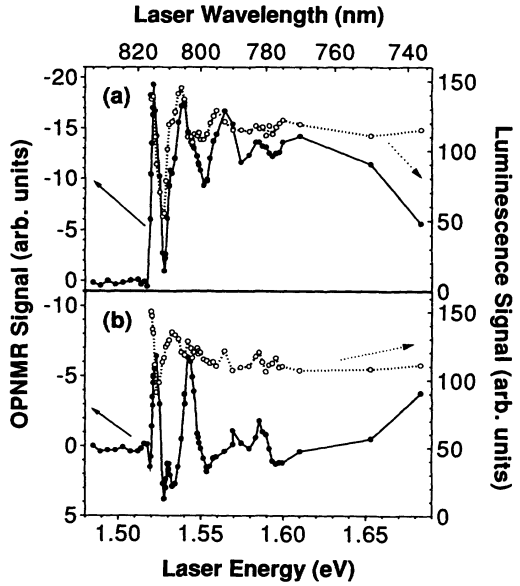


FIG. 2. Dependence of $^{71}$Ga OPNMR signal amplitude (closed circles) and PL intensity (open circles) on excitation wavelength, for $\sigma^+$ (a) and $\sigma^-$ (b) excitation. OPNMR measurements at 30 mW/cm$^2$ and 5.7 K, with $\tau_L=30$ s and $\tau_D=0$. PLE measurements at 600 mW/cm$^2$ and 5.7 K, detected at 818 nm in a crossed polarizer configuration.

cause the two techniques probe different physics. A peak in the PLE spectrum is due to optical absorption followed by carrier relaxation to a radiative state. A peak in the OPNMR spectrum is due to optical absorption followed by carrier relaxation to a nonequilibrium spin state, which need not be followed by radiative recombination.

A surprising feature of Fig. 2 is the dependence of the *sign* of the OPNMR signal on excitation wavelength for $\sigma^-$ excitation. According to previous studies of optical pumping in GaAs [3–10], the selection rules for interband transitions imply that $\sigma^+$ ($\sigma^-$) excitation generates an excess of $m=-1/2$ ($+1/2$) electrons. DNP driven by contact hyperfine couplings then generates negative (positive) nuclear polarization. Our results clearly contradict this simple picture. We also find emissive OPNMR signals for both $\sigma^+$ and $\sigma^-$ excitation in strongly *n*-doped and strongly *p*-doped *bulk* GaAs samples. In undoped or weakly doped bulk samples, however, the sign of the OPNMR signal is opposite to the helicity of the light. The high field used in our experiments may account for the unexpected behavior of the signs of the OPNMR signals through its effects on selection rules, the equilibrium polarization of electrons and holes, or relaxation processes.

Figure 3 shows the dependence of the $^{69}$Ga OPNMR signal amplitude on the laser power for various values of $\tau_L$, with $\sigma^+$ light at 815 nm, $\tau_D=0$, and $T=5.7$ K. The signal saturates above 60 mW/cm$^2$. The saturation level is independent of $T$ up to at least 13 K and is the same for $^{71}$Ga. The PL intensity does not saturate below the highest powers measured ($\sim$3 W/cm$^2$). The OPNMR signal amplitudes decrease strongly with increasing $T$ (Fig. 3, inset) but do not decrease with increasing laser power up to at least 500 mW/cm$^2$. Thus, laser heating effects are negligible.

The signal enhancement of OPNMR makes possible studies of the complex spin susceptibility [$\chi(q,\omega)$, $\omega\rightarrow 0$] of two-dimensional (2D) electron systems through directly detected measurements of NMR relaxation rates and Knight shifts [12,13]. In our sample, nuclear polarization generated in the quantum wells by optical pumping diffuses into the barriers with a diffusion constant [6] $\sim 10^{-13}$ cm$^2$/s, causing the total OPNMR signal to increase with $\tau_L$ up to $\tau_L\sim 3000$ s. By observing OPNMR signals at small or large values of $\tau_L$, we can determine NMR frequency shifts of nuclei primarily in the wells or primarily in the barriers. $^{71}$Ga shift data as a function of temperature are shown in Fig. 4. The barrier signal, observed in the dark ($\tau_L=800$ s, $\tau_D=1$ s), has a nearly temperature-independent shift of 239 ppm. The well signal in the dark ($\tau_L=5$ s, $\tau_D=1$ s) has a temperature-dependent shift $K(T)$ that can be fit by the form

$$K(T)=K_L+K\tanh(g^*\mu_B B/2kT).$$

The term $K\tanh(g^*\mu_B B/2kT)$ represents a Knight shift $K_S(T)$ proportional to the equilibrium polarization of the doped electrons. Using $K_S(T=0)=-5.7$ kHz ($-62$ ppm), based on earlier estimates of hyperfine couplings in GaAs [4], we obtain the orbital shift $K_L=242$ ppm and the effective electron $g$ value $g^*=-0.49\pm 0.02$ (solid line in Fig. 4). The derived $g^*$ is comparable to the bulk GaAs value ($g^*=-0.44$). We have also attempted to fit the shift data with a temperature-dependent $g^*$ satisfying $g^*(T)=g_0^*+g_1^*\tanh[g^*(T)\mu_B B/2kT]$, as in earlier studies of exchange-enhanced $g$ values in 2D electron systems [14–17]. *Poorer* fits result. The lack of exchange

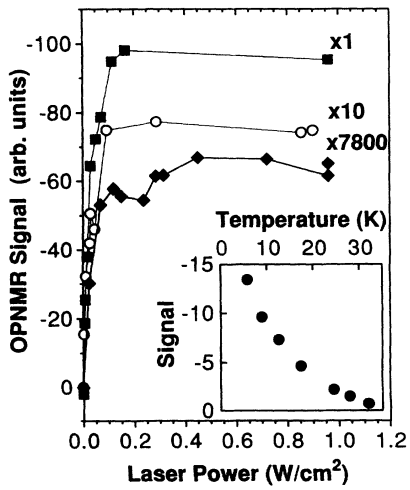


FIG. 3. Dependence of $^{69}$Ga OPNMR signal amplitude on laser power, for $\tau_L=1200$ s (filled squares), 30 s (open circles), and 0.5 s (filled diamonds). For ease of comparison, signals are scaled by the indicated factors. Inset: Dependence $^{71}$Ga OPNMR signal amplitude on temperature, for $\sigma^+$ excitation at 814 nm and 30 mW/cm$^2$, with $\tau_L=30$ s and $\tau_D=0$.

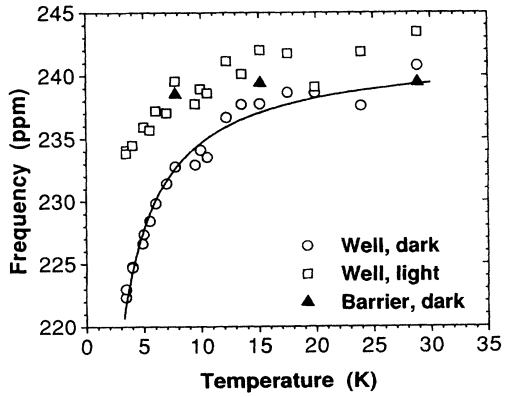


FIG. 4. Dependence of the $^{71}$Ga OPNMR frequency shift on temperature, with $\sigma^+$ excitation at 815 nm and 120 mW/cm$^2$, for nuclei in the wells observed in the dark (open circles), nuclei in the wells observed during laser excitation (open squares), and nuclei in the barriers observed in the dark (filled triangles). The solid line is a fit to the data in open circles, as explained in the text.

enhancement in our case may be due to the low electron density and low Landau filling factor ($\nu \approx 0.37$). Under light ($\tau_L = 5$ s, $\tau_D = 0$ s), the shift of the well signal changes by an amount $\Delta K(T)$ which increases with decreasing temperature. $\Delta K$ increases with the laser power only up to the saturation level discussed above. $^{69}$Ga OPNMR measurements confirm that the observed shifts are magnetic, scaling with the nuclear gyromagnetic ratio.

Approximate values of $T_1$ for nuclei in the wells can be determined from the decay of the total OPNMR signal with increasing $\tau_D$ for a fixed, small value of $\tau_L$. For $^{71}$Ga, with $\tau_L = 5$ s, we find $T_1 \sim 30$ s from 5 to 15 K. $T_1$ values determined previously by magnetoresistivity-detected NMR measurements on an $n$-doped GaAs quantum well are substantially larger [18], and may be influenced by spin diffusion.

If the spin polarizations of interacting nuclei and electrons can be described by unique nuclear and electron spin temperatures $T_n$ and $T_e$, if DNP occurs via contact hyperfine couplings, and if there is no "leakage" of nuclear polarization [1], then $T_n^{-1} - T^{-1} = (\varepsilon_e/\varepsilon_n)(T_e^{-1} - T^{-1})$ at steady state, where $\varepsilon_e$ and $\varepsilon_n$ are the electron and nuclear Zeeman energies. In Fig. 1(a), $T_n \approx -170$ mK, implying $T_e - T \approx 0.3$ K for $g^* = -0.49$ (assuming that steady state is reached in the wells at $\tau_L = 30$ s). However, the observed $\Delta K$ values imply $T_e - T \approx 4$ K. Thus, we are led to propose that the photoexcited electrons may not reach a common spin temperature with the doped electrons. For example, our data can be explained by assuming that, under laser irradiation above saturation at $T \approx 5$ K, the nuclei couple to doped electrons with $T_e \approx 5$ K and $n_s = 6.3 \times 10^{10}$ cm$^{-2}$ and to photoexcited electrons with $g^* \mu_B B/k < T_e^* < 0$ and $n_s^* \sim 1 \times 10^{10}$ cm$^{-2}$. $T_n$ would then be determined by the competing couplings to doped and photoexcited electrons. Such a large value of $n_s^*$, together with the small value of the saturation power, necessitates excitation lifetimes and electron spin relaxation times of $\sim 1$ $\mu$s. The relevant excitations may be long-lived, "dark" magnetoexcitons [19,20] (i.e., excitons composed of occupied $m = 1/2$ conduction band and vacant $m = -3/2$ valence band states). The apparent decoupling of the electron spin temperatures in this picture is not understood, but may be a consequence of the high magnetic field.

Directly detected OPNMR has several advantages over ODNMR, in that polarized luminescence is not required, high magnetic fields can be used, pulsed NMR techniques (e.g., multiple pulse sequences, double-resonance methods, multidimensional spectroscopy) can be adopted without modification, and nuclei that are far from the optically absorptive region or make negligible contributions to the total nuclear hyperfine fields can be observed. In future work, we plan to exploit OPNMR in studies of the structural and electronic properties of semiconductor thin films and heterostructures and to explore the generality of OPNMR in other materials classes.

We thank T. D. Harris, J. P. Eisenstein, S. K. Buratto, and G. Dabbagh for useful advice and experimental assistance.

[1] A. Abragam, *Principles of Nuclear Magnetism* (Oxford Univ. Press, New York, 1961).
[2] G. Lampel, Phys. Rev. Lett. **20**, 491 (1968).
[3] *Optical Orientation*, edited by F. Meier and B. P. Zakharchenya (Elsevier, Amsterdam, 1984).
[4] D. Paget, G. Lampel, B. Sapoval, and V. I. Safarov, Phys. Rev. B **15**, 5780 (1977).
[5] D. Paget, Phys. Rev. B **24**, 3776 (1981).
[6] D. Paget, Phys. Rev. B **25**, 4444 (1982).
[7] G. P. Flinn, R. T. Harley, M. J. Snelling, A. C. Tropper, and T. M. Kerr, Semicond. Sci. Technol. **5**, 533 (1990).
[8] V. K. Kalevich, V. L. Korenev, and O. M. Fedorova, Pis'ma Zh. Eksp. Teor. **52**, 964 (1990) [JETP Lett. 52, 349 (1990)].
[9] M. Krapf, G. Denninger, H. Pascher, G. Weimann, and W. Schlapp, Solid State Commun. **78**, 459 (1991).
[10] S. K. Buratto, D. N. Shykind, and D. P. Weitekamp, Phys. Rev. B **44**, 9035 (1991).
[11] M. Altarelli, in *Heterojunctions and Semiconductor Superlattices*, edited by G. Allan, G. Bastard, N. Boccara, M. Lannoo, and M. Voos (Springer-Verlag, New York, 1986).
[12] J. Winter, *Magnetic Resonance in Metals* (Oxford Univ. Press, New York, 1971).
[13] I. D. Vagner and T. Maniv, Phys. Rev. Lett. **61**, 1400 (1988).
[14] T. Englert, D. C. Tsui, A. C. Gossard, and C. Uihlein, Surf. Sci. **113**, 295 (1982).
[15] R. J. Nicholas, R. J. Haug, K. von Klitzing, and G. Weimann, Phys. Rev. B **37**, 1294 (1988).
[16] A. Usher, R. J. Nicholas, J. J. Harris, and C. T. Foxon, Phys. Rev. B **41**, 1129 (1990).
[17] T. Ando and Y. Uemura, J. Phys. Soc. Jpn. **37**, 1044 (1974).
[18] A. Berg, M. Dobers, R. R. Gerhardts, and K. von Klitzing, Phys. Rev. Lett. **64**, 2563 (1990).
[19] J. B. Stark, W. H. Knox, and D. S. Chemla, Phys. Rev. B **46**, 7919 (1992).
[20] S.-R. E. Yang, and L. J. Sham, Phys. Rev. Lett. **58**, 2598 (1987).